

In-situ Broadband Cryogenic Calibration for Two-port Superconducting Microwave Resonators

Jen-Hao Yeh^{1,2, a)} and Steven M. Anlage^{1,2}

¹⁾ *Electrical and Computer Engineering Department, University of Maryland, College Park, Maryland 20742-3285*

²⁾ *CNAM, Physics Department, University of Maryland, College Park, Maryland 20742-4111*

(Dated: 19 December 2012)

In this paper we introduce an improved microwave calibration method for use in a cryogenic environment, based on a traditional three-standard calibration, the Thru-Reflection-Line (TRL) calibration. The modified calibration method takes advantage of additional information from multiple measurements of an ensemble of realizations of a superconducting resonator, as a new pseudo-Open standard, to correct errors in the TRL calibration. We also demonstrate an experimental realization of this *in-situ* broadband cryogenic calibration system utilizing cryogenic switches. All calibration measurements are done in the same thermal cycle as the measurement of the resonator (requiring only an additional 20 minutes), thus avoiding 4 additional thermal cycles for traditional TRL calibration (which would require an additional 12 days). The experimental measurements on a wave-chaotic microwave billiard verify that the new method significantly improves the measured scattering matrix of a high-quality-factor superconducting resonator.

PACS numbers: 84.40.-x, 07.20.Mc, 06.20.fb, 06.30.Ka, 07.57.Pt, 05.45.Mt

I. INTRODUCTION

Microwave resonators are widely-utilized devices in many science and engineering fields. In order to achieve very low dissipation and attain extremely high quality factors Q , microwave resonators can be made of superconducting materials at temperatures lower than the critical temperature T_c ^{1,2}. One important application of superconducting resonators is in building particle accelerators. Because superconducting resonators can store energy with very low loss and a narrow bandwidth, they can transfer this energy to a charged particle beam with high efficiency³.

Another application of superconducting resonators, and also the motivation of the microwave calibration method in this paper, is to test the predictions of wave chaos theories in a low loss (nearly unitary) regime⁴. Wave chaos, or quantum chaos⁵, is a field where researchers study the manifestations of chaotic dynamics of classical trajectories on the short-wavelength (quantum or wave) properties of wave systems. Random Matrix Theory (RMT)⁶ has successfully been applied to predict many statistical properties of open wave-chaotic systems, such as the scattering matrices (S), the impedance matrices (Z), the conductivities, and the fading amplitudes^{4,7-12} in complicated wave scattering environments. There has been great success in studying the properties of wave chaotic systems in the context of microwave billiards⁵.

For the scattering matrix S of an open wave scattering system, the prediction of RMT is for the *universal* features of the statistical distributions of the elements of S

and their correlations, which should only depend on the loss parameter of the system⁷⁻¹⁰. The loss parameter α is defined as the ratio of the 3dB-frequency bandwidth of the cavity resonances due to distributed losses, to the average spacing between resonant frequencies, and it can be quantified by the expression $\alpha = k^2/(\Delta k_n^2 Q)$ where k is the wave number for the incoming wave, Δk_n^2 is the mean spacing of the adjacent eigenvalues of the Helmholtz operator ($\nabla^2 + k^2$) of the corresponding closed system, and Q is the loaded quality factor of the cavity^{8,9}. Note that the system-specific (*non-universal*) features of the wave scattering properties can be removed by methods such as the random coupling model (RCM)^{9,11,13,14} or the Poisson Kernel¹⁵. Examination of these predictions in very low loss systems is interesting because extreme limits for the distribution functions and other predictions are encountered^{7,8,12}. For example, in a two-port system, the distributions of the magnitude of $|S_{21}|$ are similar to a Rayleigh distribution with moderate and high loss parameters, but the distribution $P(|S_{21}|)$ goes to a uniform distribution when the loss parameter goes to zero in a time-reversal invariant system^{7,12}. In order to test these statistical predictions, we use a two-port superconducting microwave resonator as the wave-chaotic cavity to create a low-loss experimental system, and we measure the 2×2 scattering matrix S of the cavity in a wide frequency band.

To measure the scattering matrix S with high accuracy over a broad bandwidth, a broadband calibration method of microwave measurement is necessary. The calibration method removes the effect of the transmission lines connecting the vector network analyzer (VNA) at room temperature and the cryogenic sample at low temperature. Because the convenient electronic-calibration kit of a commercial VNA does not function in a cryogenic environment, one has to perform a manual calibration by

^{a)} davidyeh@umd.edu

utilizing known standards.

II. REVIEW OF CRYOGENIC MICROWAVE CALIBRATION

Microwave calibration is an important process to remove the systematic errors due to the transmission lines between the network analyzer and the device under test (DUT) as well as other systematic measurement errors. The calibration process uses measurements of known standards to move the measurement reference plane to the ports of the DUT^{16,17}. A commonly-used calibration method for two-port measurement is a multiple-standard calibration, the Thru-Reflection-Line (TRL) calibration^{18,19}.

The TRL calibration uses three standards to calibrate the effect of the two transmission lines connecting the VNA to the DUT. For calibration standards, the two transmission lines are directly connected together for the Thru standard measurement; an additional electrically short (on the order of one guided wavelength) transmission line is added between the two transmission lines as the Line standard; two identical reflectors are connected to the ends of the two transmission lines as the Reflection standard¹⁹. The advantages of the TRL calibration are from two facts: (i) the use of redundant calibration standards reduces the uncertainty due to errors, such as connector irreproducibility, cable flexure, test-set drift, and noise, and (ii) the foundation of the calibration standard definitions depend solely on qualitative requirements (uniformity of the lines, identical cross-sections of the lines, and identical reflection coefficients of the Reflection standards)²⁰.

For cryogenic calibration, measuring multiple standards involves cool down and warm up of the system, changing the standard, and repeating the thermal cycle. These thermal cycles can be very time consuming and expensive. In addition, there is enhanced uncertainty of reproducibility of experimental conditions^{17,20}. On the other hand, researchers have developed single-thermal-cycle calibration methods which use an on-wafer cryogenic probe station or electromechanical switches. However, the problem with this method is that the differences between electrical paths in measurements of different standards, which are assumed to be equal, degrade the measurement accuracy and limit the frequency bandwidth¹⁷.

A pioneering work on broadband cryogenic calibration of a one-port system was done by Booth *et al.*²¹ who measured the complex reflection coefficient S_{11} of a superconducting thin film. They cooled the sample deep into the superconducting state and used it as a short-circuit standard to correct their room temperature calibration of the Corbino reflectometer. Reuss and Richard²² also measured broadband S_{11} of a superconducting thin film by applying the 3-standard (Open, Short, Load) calibration, once at the room temperature and once at the super-

conducting temperature. Other researchers also applied this Open-Short-Load (OSL) calibration and the Corbino approach in their one-port cryogenic measurement^{23–25}. One problem of the OSL calibration is that it is very sensitive to the standards, and one must carefully reproduce all connections, bending and twisting of the transmission lines, and the temperature distribution in the apparatus^{21–24}. Kitano *et al.*²⁶ used the normal-state conductivity of a sample as a Load standard to address this problem.

For two-port systems, researchers have developed cryogenic TRL calibration methods for measurement of the 2×2 scattering matrices of the DUT. Laskar *et al.*²⁷ utilized the multiline method of the TRL and LRM (Line-Reflection-Match) calibrations introduced by Marks¹⁹, to their cryogenic on-wafer probe station for noise and scattering-parameter measurements, and they emphasized the importance of providing a stable thermal environment²⁷. Booth *et al.* also used a vector network analyzer and a cryogenic probe station for scattering-parameter measurements of their coplanar waveguide (CPW) structures in high temperature superconductors^{28,29}. In addition, they applied a set of CPW calibration structures of TRL standards to characterize the errors in the network analyzer/probe station system²⁸, or alternatively three other standards: a Thru, a Reflection, and a series resistor³⁰.

Another way to achieve single-thermal-cycle TRL calibration is to utilize cryogenic microwave switches. Ranzani *et al.*³¹ use cryogenic switches (coaxial subminiature latching switches) to switch the VNA to different calibration standards, as well as the device under test. The electromechanical switches operate by means of brief electrical pulses to latch the switch to different positions, so no electrical signal is applied to the switch in its quiescent state. Similar cryogenic switches have been applied for calibrating measurement of Superconducting Quantum Interference Device (SQUID) amplifiers³², measuring different superconducting qubit samples³³, or other experiments involving superconducting quantum computing³⁴. Due to the convenience of connecting the coaxial transmission lines to the ports of our superconducting cavity, we use cryogenic switches to develop our *in-situ* calibration system.

Although the TRL calibration is less sensitive to the properties of the standards than the OSL calibration, the TRL calibration is still limited by errors in its assumptions, such as irreproducibility of the transmission lines in each measurement, differences in the reflection coefficients of the two reflectors, and irreproducibility of the connector interface^{20,35}. Researchers have tried different methods to reduce the calibration errors, such as the development of precise dimensional characterization techniques for the transmission lines³⁶, the minimization of the possible center-conductor-gap variation³⁷, and modeling of the electrical properties combined with self-calibration approaches^{20,38}. In our cryogenic measurements, the temperature dependence of the scattering ma-

trices of all transmission lines and imperfect TRL standards become additional sources of errors. These small errors are especially significant in our extremely-low loss system because the calibrated $|S_{11}|$ and $|S_{22}|$ are very close to 1 away from the resonance frequencies.

In this paper, we introduce a self-calibration approach by taking advantage of multiple measurements in different realizations of the superconducting resonator. We call this additional information a pseudo-Open standard and utilize it to correct the measured scattering matrices. With the improvement provided by the pseudo-Open standard, we also demonstrate an experimental result utilizing this *in-situ* broadband cryogenic calibration system.

III. CALIBRATION METHOD

A. The Superconducting Resonator

We have carried out experiments by measuring the complex 2×2 scattering matrix S of a quasi-two-dimensional microwave cavity, illustrated in Fig. 1. There are two coupling ports (the red cylinders and dots in Fig. 1) where microwaves are injected through an antenna attached to a single-mode coaxial transmission line of characteristic impedance $Z_0 = 50 \Omega$. Each antenna is inserted into the cavity through a small hole in the lid, similar to previous setups^{9,12}. The waves introduced have frequencies from 6 to 18 GHz, and they are quasi-two-dimensional due to the thin height of the cavity (8 mm in the z direction). The antennas are terminated with SMA connectors, one male and the other female, on the surface of the resonator. The shape of the cavity is a “cut-circle” and is a billiard potential that shows classical chaos^{12,39–41}.

The superconducting cavity is made of copper with Pb-plated walls and cooled to a temperature (6.6 K) below the transition temperature of Pb^{40–42}. Measurements of the transmission spectrum suggest that the quality factor of the resonances is on the order of $Q \approx 10^5$. A Teflon wedge (the blue wedge in Fig. 1) can be rotated as a ray-splitting perturber inside the cavity, and we rotate the wedge by 5° each time to create 72 different ensemble realizations. The rotation axis of the perturber is connected with a MDC vacuum rotary feedthrough (BRM-133) at room temperature, so we can control the angular position from outside the cryostat. The original purpose of creating these realizations was to gather statistics to test the statistical predictions of RMT, but it is now a critical procedure for the pseudo-Open standard.

B. The In-situ Broadband Cryogenic Calibration System

Figure 2 shows the setup of our *in-situ* broadband cryogenic calibration system. The term “*in-situ*” means

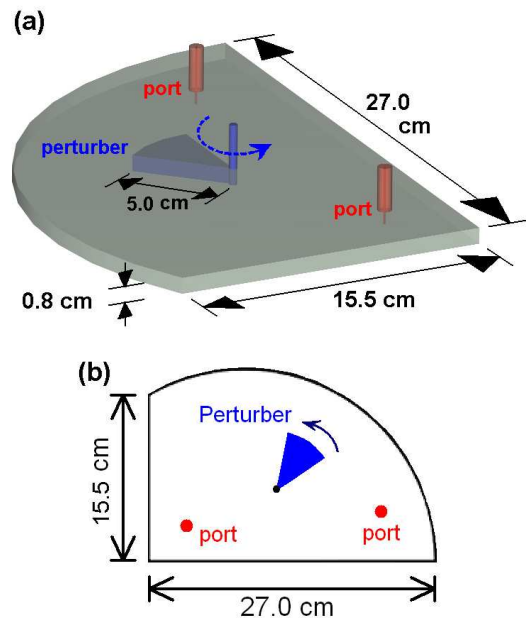


FIG. 1. (a) The quasi-two-dimensional cut-circle microwave cavity in a three-dimensional perspective, showing the cavity dimensions, ports, and the perturber. (b) Projected two-dimensional view of the cut-circle billiard.

the TRL calibration process can be applied at low temperatures without spending a great deal of time changing standards. Here we utilize two cryogenic 6-position switches (Radiall coaxial subminiature latching switches R591722605) to include one Thru, one Reflection, and two Line standards together with the cavity under measurement. Each switch is connected to different standards, or to the cavity, by RF COAX phase-matched (13 inch long between interfaces, electrical length deviations < 1 ps) SMA coaxial cables (S086MMHF-013-1). For the Thru standard, we directly connect the pair of coaxial cables. For the Reflection standard, we use two short circuits (Fairview Microwave models SC2136 and SC2141) to terminate the pair of coaxial cables. For the Line standards, we add two different SMA male-to-female adapters (of electrical length 1.94 cm and 2.56 cm) to connect the two pairs of coaxial cables, one with a male interface and the other with a female interface. All of these standards and the cut-circle cavity are at a uniform temperature in the cryostat, and the switches are controlled by voltage pulses from a DC power supply (Hewlett-Packard E3610A) outside the cryostat. The network analyzer is an Agilent Technologies E8364C.

The cryostat includes two cylindrical vacuum chambers (aluminum) with one cylindrical thermal shield (copper) in between them. The switches, calibration standards, and the superconducting resonator are all contained in the inner vacuum chamber (designed temperature 4 K, radius 16.5 cm, and height 30.2 cm). We use an Alcatel Drytel 31 Dry Vacuum Pump System to evacuate the inner and outer chambers to a pressure lower than

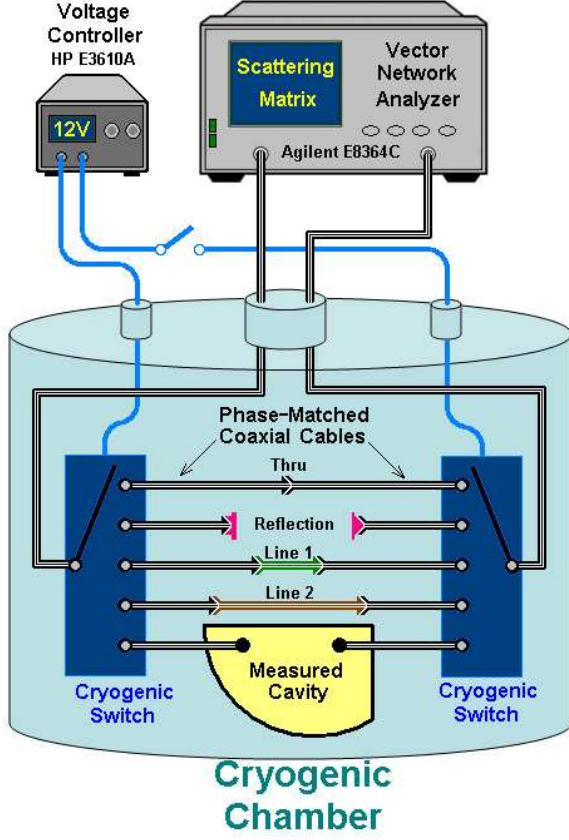


FIG. 2. Experimental setup of the *in-situ* broadband cryogenic calibration system. The phase-matched coaxial cables have nearly identical length and are not shown to scale.

1×10^{-6} atm and a Cryomech PT405 Pulse Tube Cryorefrigerator (with a water-cooled compressor) to cool down the resonator to the base temperature of 6.6 K. The resonator is hung on the cold plate of the Cryorefrigerator, and we also use copper thermal straps to connect the cold plate and the resonator. The thermometer is attached in the lower part of the outside surface of the resonator. We also designed two copper clamps to mount the cryogenic switches on the cold plate. The second layer of the cryostat is the cylindrical copper shield (designed temperature 40 K, radius 17.8 cm, and height 43.8 cm). The third layer is the outer vacuum chamber (designed temperature 300 K, radius 20.3 cm, and height 55.9 cm). For a thermal cycle, it takes about one day to pump the system to vacuum and cool down the resonator to thermal equilibrium at the base temperature, while warming-up takes about two days. The dwell time of the system at the base temperature can be longer than one week.

One advantage of using cryogenic switches is to save a great deal of time for the TRL calibration. One full thermal cycle of this cryostat takes about 3 days, so a multiple-thermal-cycle TRL calibration for 4 standards would require an additional 12 days for calibration. However, with the *in-situ* calibration system, we only need an additional 20 minutes for measuring the 4 standards

within the same thermal cycle for measuring the superconducting cavity.

The cryogenic switches also make the calibration process conveniently accessible each time the system environment is modified, for example, by changing the temperature, microwave power, or external magnetic field. We can adjust the equilibrium temperature of the cavity and standards by tuning the applied DC current to heating resistors installed in the cryostat. The applied microwave power can be controlled by the network analyzer. In addition to increasing the efficiency of the experiment, avoiding opening/closing the chamber for changing standards also reduces the uncertainties created by having different temperatures or different layouts of transmission lines in each measurement.

On the other hand, the disadvantage of using cryogenic switches is that the switches utilize 5 different pairs of transmission lines to connect to the standards or the cavity. The differences of the scattering matrices of these electrical paths are additional errors of the TRL calibration. We have measured the differences at room temperature, and the deviations from the switches are $|\Delta S| < 0.01$; the deviations from the transmission lines are $|\Delta S| < 0.06$. These errors can be reduced from the calibrated results by the pseudo-Open standard introduced in the following section.

The calibration system is also broadband because we install two Line standards. The TRL calibration is invalid for frequencies where the phase difference between the Thru standard and the Line standard is too small (the phase difference should be greater than 20 degrees and less than 160 degrees)^{16,19}. To solve this problem, one can use two Line standards with different lengths and make sure that the problematic frequency bands do not overlap. Therefore, we use the cryogenic switches to connect two different Line standards to achieve broadband calibration, for example, we can measure the scattering matrix continuously from 3 to 21 GHz.

C. Pseudo-Open Standard

The original TRL calibration still has many errors, such as the irreproducibility of the transmission lines and connectors in each measurement, the difference between the two reflectors in the Reflection standard, and the impedance-mismatch of the connectors between the Thru and Line standards. These errors are especially critical when $|S_{11}|$ and $|S_{22}|$ of the measured cavity are close to 1. In our case, while the frequency is away from the resonant frequencies of the superconducting resonator, $|S_{11}|$ and $|S_{22}|$ are very close to 1 (i.e. the transmission coefficient $|S_{21}|$ is very close to 0, and there is almost no absorption in the cavity) in the extremely low loss environment. Therefore, a small error can make $|S_{11}|$ or $|S_{22}|$ larger than 1 and cause non-physical results. This small error is also critical for analysis of the 2×2 impedance matrix Z , obtained by a bilinear transforma-

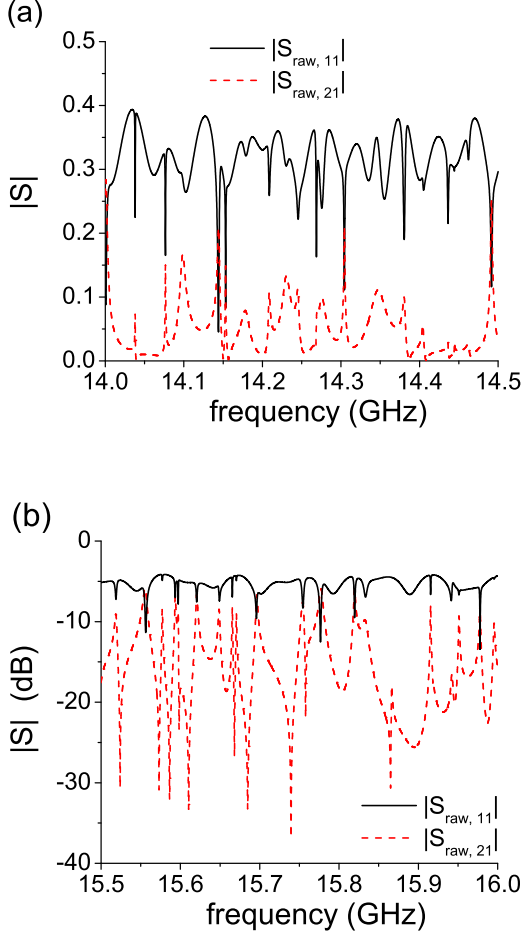


FIG. 3. The magnitude of raw measured scattering matrix element S_{11} (black solid curves) and S_{21} (red dash curves) versus frequency for the superconducting cut-circle microwave cavity at 6.6 K. (a) An example with the frequency band from 14.0 to 14.5 GHz plotted in linear scale; (b) another example with the frequency band from 15.5 to 16.0 GHz plotted in semi-logarithmic scale.

tion as $Z = Z_0(I_2 + S)/(I_2 - S)$ where Z_0 is the diagonal characteristic impedance matrix of the transmission lines (50Ω) and I_2 is a 2×2 identity matrix. The denominator ($I_2 - S$) makes the impedance matrix sensitive to this small error when S_{11} or S_{22} are close to 1.

Figure 3 shows two examples of the raw data (no calibration) of the magnitude of the scattering matrix element versus frequency. Because the loss parameter in the superconducting resonator is very low ($\alpha \ll 1$, i.e. high Q), the curves of $|S_{raw,11}|$ and $|S_{raw,21}|$ show sharp and well-separated resonances on a smoothly varying background. Note that all degeneracies are broken in wave chaotic systems⁵. The background feature shows the influence of the transmission lines between the cavity and the network analyzer, and this is what we want to remove by calibration. With the cryogenic TRL calibration, we

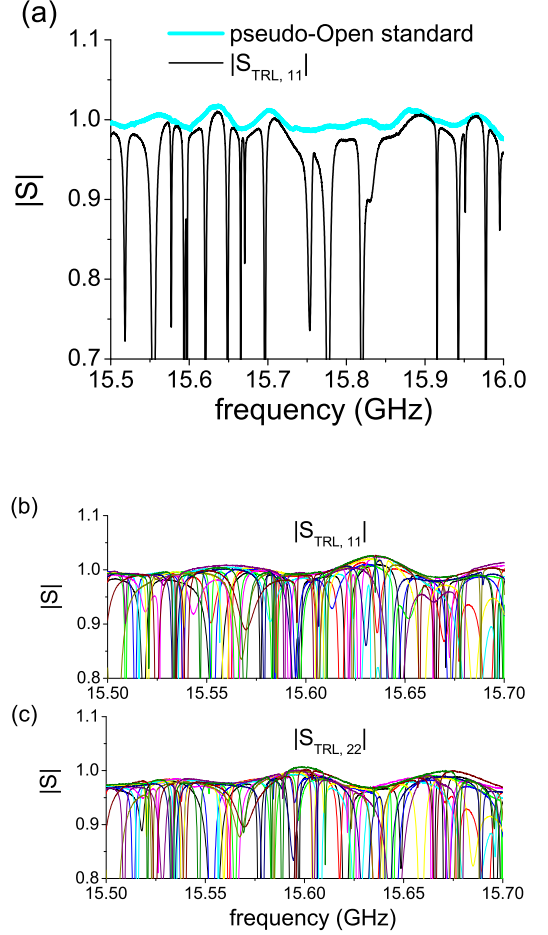


FIG. 4. (a) The magnitude of TRL-calibrated S_{11} (the black curve) and the pseudo-Open standard (the thicker light-blue curve) versus frequency. Shown are 12 realizations of the magnitude of TRL-calibrated (b) S_{11} and (c) S_{22} in varied colors versus frequency.

can eliminate most of the influence from the transmission lines, and the result of TRL-calibrated $|S_{TRL,11}|$ is shown as the black curve in Fig. 4(a). Now $|S_{TRL,11}|$ is close to 1 off of the resonant frequencies as we expect for a superconducting resonator. However, there are still small fluctuations in the background due to the systematic errors of the TRL calibration. Note that at some frequencies (e.g. near 15.64 GHz), the small error makes $|S_{TRL,11}| > 1$.

To solve this problem, we introduce the pseudo-Open standard by taking advantage of the 72 ensemble realizations of the cavity. For each realization, we only change the orientation of the Teflon perturber, and all of the other features, including the transmission lines, cavity volume, etc., remain the same. Therefore, by comparing the measured data of the 72 realizations, the scattering matrices in all realizations have similar background curves, but the well-separated and narrow resonances are

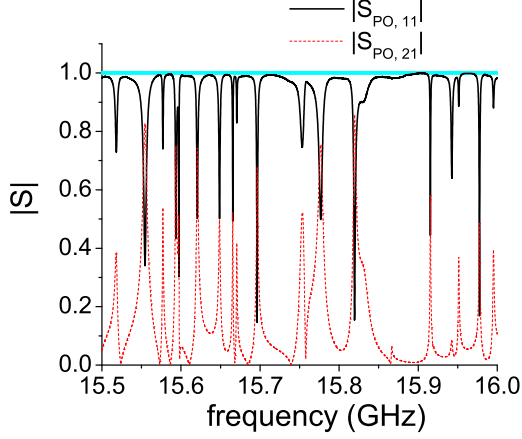


FIG. 5. The magnitude of TRL-calibrated and pseudo-Open-corrected S_{11} (the black solid curve) and S_{21} (the red dash curve) versus frequency.

moved to various frequencies. For illustration, Fig. 4(b) and Fig. 4(c) show $|S_{TRL,11}|$ and $|S_{TRL,22}|$ in 12 realizations (each for a perturber orientation 30° apart). Note that the peak values of $|S_{TRL,11}|$ and $|S_{TRL,22}|$ form a systematic oscillating background, which is the feature of a combination of all errors of the TRL calibration. In order to utilize this feature, we exclude all resonances by considering the maximum values of $(|S_{TRL,11}|^2 + |S_{TRL,21}|^2)$ and $(|S_{TRL,22}|^2 + |S_{TRL,12}|^2)$. We note that $(|S_{TRL,11}|^2 + |S_{TRL,21}|^2)$ and $(|S_{TRL,22}|^2 + |S_{TRL,12}|^2)$ are unity in a lossless system. Thus, we define a diagonal matrix O_p , where $O_{p,11}$ is the maximum of $\sqrt{|S_{TRL,11}|^2 + |S_{TRL,21}|^2}$ over all realizations, and $O_{p,22}$ is the maximum of $\sqrt{|S_{TRL,22}|^2 + |S_{TRL,12}|^2}$ over all realizations. In a very low loss system, O_p should be close to an identity matrix if the TRL calibration has no error, so the fluctuations of O_p represent the remaining errors. We call O_p the pseudo-Open standard because O_p is like an Open standard when we exclude all resonances (i.e. no energy is transmitted through the two ports). Figure 4(a) shows the pseudo-Open standard response $O_{p,11}$ as the thicker light-blue curve. By utilizing the information from multiple measurements of the cavity in different realizations, the pseudo-Open standard helps to calibrate out the errors due to the deviations between the transmission lines connected to the TRL standards and the transmission lines connected to the cavity.

We simply remove the errors and obtain a TRL-calibrated and pseudo-Open-corrected scattering matrix S_{PO} by

$$S_{PO} = S_{TRL} O_p^{-1}. \quad (1)$$

Figure 5 shows the result of the pseudo-Open correction. The small systematic fluctuation in the TRL-calibrated data $|S_{TRL,11}|$ is removed after applying the pseudo-Open standard. Therefore, by using the TRL calibra-

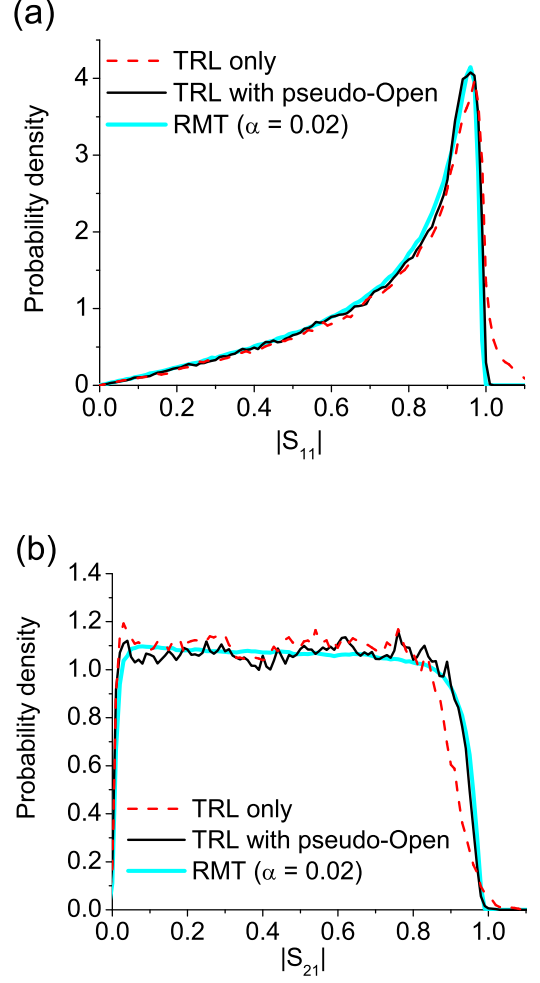


FIG. 6. The probability density of (a) $|S_{11}|$ and (b) $|S_{21}|$ of the RMT predictions (thicker light-blue curves), the experimental data from the superconducting cut-circle cavity at 6.6 K with TRL-calibration (red dash curves), and the data with TRL-calibration and pseudo-Open correction (black curves).

tion with the pseudo-Open standard, we can have well-calibrated data of the scattering matrix, and we are able to do further analysis of the statistics of the scattering matrices or the impedance matrices for wave chaos research¹².

D. Results and Test of RMT Predictions

With the well-calibrated data of the scattering matrix, we can now apply the random coupling model^{8,9,11,14} to remove the system-specific features of the scattering matrix and reveal the universal statistics which are predicted by Random Matrix Theory^{7,12}. Figure 6 shows a comparison of the predictions of RMT (thicker light-blue curves) and the experimental data which are calibrated

with cryogenic TRL calibration only (red dash curves) and also with pseudo-Open correction (black curves) for the statistics of RCM-normalized $|S_{11}|$ and $|S_{21}|$. The probability density functions (PDF) of the experimental data are taken from all 72 realizations and in frequency from 14.0 to 16.0 GHz. The RMT prediction is the best-matched PDF with a single parameter (the loss parameter α), and $\alpha = 0.02$ is the fit value. The results show that the pseudo-Open correction makes significant improvement in the PDFs when $|S_{11}|$ or $|S_{21}|$ are close to 1. The non-physical features ($|S| > 1$, seen in the TRL calibrated data in Fig. 4(a)) are almost entirely eliminated with the addition of the pseudo-Open standard. One can generalize these results to other resonant systems in which the modes can be perturbed by external means, such as strain, electric field, temperature, magnetic field, etc.

IV. CONCLUSION

Superconducting microwave resonators are useful devices in many applications, and well-calibrated measurement of their scattering matrices is beneficial. In this paper we demonstrate an *in-situ* broadband cryogenic calibration system where the calibration process is made dramatically more convenient by installing two cryogenic switches for single-thermal-cycle TRL calibration. We also introduce a pseudo-Open standard by taking advantage of the ensemble realizations of the superconducting cavity with a movable perturber and the feature of well-separated resonances in an extremely low loss environment. Experimental data verify that the pseudo-Open standard can significantly improve the TRL-calibrated data. We show that the well-calibrated scattering matrices are beneficial for wave chaos research, and this work should broadly benefit various applications related to high-precision cryogenic measurement.

ACKNOWLEDGMENTS

We thank the group of A. Richter (Technical University of Darmstadt) for graciously loaning the cut-circle billiard, and H. J. Paik and M. V. Moody for use of the pulsed tube refrigerator. We also acknowledge L. Ranzani for introducing us to the cryogenic switches. This work is funded by the ONR/Maryland AppEl Center Task A2 (Contract No. N000140911190), the AFOSR under Grant No. FA95500710049, NSF-GOALI ECCS-1158644, and the Center for Nanophysics and Advanced Materials (CNAM).

¹H. Weinstock and M. Nisenoff, *Microwave Superconductivity*, (Kluwer Academic Publishers, Dordrecht, Netherlands, 1999).

²M. A. Hein, *High-Temperature-Superconductor Thin Films at Microwave Frequencies*, (Springer Tracts in Modern Physics **155**, Springer, Heidelberg, Germany, 1999).

³H. Padamsee, J. Knobloch, and T. Hays, *RF Superconductivity for Accelerators*, (John Wiley & Sons, New York, 1998).

⁴H.-D. Gräf, H. L. Harney, H. Lengeler, C. H. Lewenkopf, C. Rangacharyulu, A. Richter, P. Schardt, and H. A. Weidenmüller, *Phys. Rev. Lett.* **69**, 1296 (1992); H. Alt, C. I. Barbosa, H.-D. Gräf, T. Guhr, H. L. Harney, R. Hofferbert, H. Rehfeld, and A. Richter, *Phys. Rev. Lett.* **81**, 4847 (1998); C. Dembowski, B. Dietz, T. Friedrich, H.-D. Gräf, A. Heine, C. Mejía-Monasterio, M. Miski-Oglu, A. Richter, and T. H. Seligman, *Phys. Rev. Lett.* **93**, 134102 (2004); A. Y. Abul-Magd, B. Dietz, T. Friedrich, and A. Richter, *Phys. Rev. E* **77**, 046202 (2008); B. Dietz, T. Friedrich, H. L. Harney, M. Miski-Oglu, A. Richter, F. Schäfer, and H. A. Weidenmüller, *Phys. Rev. E* **81**, 036205 (2010).

⁵H.-J. Stöckmann, *Quantum Chaos*, (Cambridge University Press, Cambridge, England, 1999).

⁶M. L. Mehta, *Random Matrices*, 2nd ed. (Academic Press, Boston, 1991); G. Akemann, J. Baik, and P. Di Francesco, *The Oxford Handbook of Random Matrix Theory*, (Oxford University Press, New York, 2011).

⁷P. W. Brouwer and C. W. J. Beenakker, *Phys. Rev. B* **55**, 4695 (1997); C. W. J. Beenakker, *Rev. Mod. Phys.* **69**, 731 (1997); Y. Alhassid, *Rev. Mod. Phys.* **72**, 895 (2000).

⁸X. Zheng, T. M. Antonsen Jr., E. Ott, *Electromagnetics* **26**, 3 (2006); *Electromagnetics* **26**, 37 (2006).

⁹S. Hemmady, X. Zheng, E. Ott, T. M. Antonsen, and S. M. Anlage, *Phys. Rev. Lett.* **94**, 014102 (2005); *Phys. Rev. E* **71**, 056215 (2005); *Phys. Rev. E* **74**, 036213 (2006); S. Hemmady, J. Hart, X. Zheng, T. M. Antonsen, E. Ott, S. M. Anlage, *Phys. Rev. B* **74**, 195326 (2006).

¹⁰Y. V. Fyodorov, D. V. Savin, and H.-J. Sommers, *J. Phys. A: Math. Gen.* **38**, 10731 (2005).

¹¹J.-H. Yeh, J. Hart, E. Bradshaw, T. Antonsen, E. Ott, and S. M. Anlage, *Phys. Rev. E* **82**, 041114 (2010).

¹²J.-H. Yeh, T. M. Antonsen, E. Ott, and S. M. Anlage, *Phys. Rev. E* **85**, 015202 (2012).

¹³M. Lawniczak, O. Hul, S. Bauch, P. Seba, and L. Sirko, *Phys. Rev. E* **77**, 056210 (2008); M. Lawniczak, S. Bauch, O. Hul, and L. Sirko, *Phys. Scr.* **T147**, 014018 (2012).

¹⁴S. Hemmady, T. M. Antonsen, E. Ott, S. M. Anlage, *IEEE Trans. Electromag. Compat.* **54**, 758 (2012).

¹⁵P. A. Mello, P. Pereyra, and T. H. Seligman, *Ann. Phys.* **161**, 254 (1985); J. Stein and H.-J. Stöckmann, *Phys. Rev. Lett.* **68**, 2867 (1992); Y.-H. Kim, M. Barth, U. Kuhl, H.-J. Stöckmann, and J. P. Bird, *Phys. Rev. B* **68**, 045315 (2003); U. Kuhl, M. Martínez-Mares, R. A. Méndez-Sánchez, and H.-J. Stöckmann, *Phys. Rev. Lett.* **94**, 144101 (2005).

¹⁶http://na.tm.agilent.com/pna/help/latest/S3-Cals/TRL_Calibration.htm.

¹⁷J. L. Cano de Diego, Ph.D. thesis, University of Cantabria, 2010.

¹⁸G. F. Engen and C. A. Hoer, *IEEE Trans. Microw. Theory Tech.* **27**, 987 (1979).

¹⁹R. B. Marks, *IEEE Trans. Microw. Theory Tech.* **39**, 1205 (1991).

²⁰A. Lewandowski and W. Wiatr, *74th ARFTG Microwave Measurement Symposium*, Broomfield, Colorado, 2009 (DOI: 10.1109/ARFTG74.2009.5439110).

²¹J. C. Booth, D. H. Wu, and S. M. Anlage, *Rev. Sci. Instrum.* **65**, 2082 (1994); J. C. Booth, D. H. Wu, S. B. Qadri, E. F. Skelton, M. S. Osofsky, A. Piqué, and S. M. Anlage, *Phys. Rev. Lett.* **77**, 4438 (1996).

²²T. Reuss and J. Richard, *IEEE Trans. Microw. Theory Tech.* **48**, 1286 (2000).

²³M. L. Stutzman, M. Lee, and R. F. Bradley, *Rev. Sci. Instrum.* **71**, 4596 (2000).

²⁴M. Scheffler and M. Dressel, *Rev. Sci. Instrum.* **76**, 074702 (2005).

²⁵K. Steinberg, M. Scheffler, and M. Dressel, *Rev. Sci. Instrum.* **83**, 024704 (2012).

²⁶H. Kitano, T. Ohashi, and A. Maeda, *Rev. Sci. Instrum.* **79**, 074701 (2008).

²⁷J. Laskar, J. J. Bautista, M. Nishimoto, M. Hamai, and R. Lai, *IEEE Trans. Microw. Theory Tech.* **44**, 1178 (1996).

²⁸J. C. Booth, J. A. Beall, D. C. DeGroot, D. A. Rudman, R. H. Ono, J. R. Miller, M. L. Chen, S. H. Hong, and Q. Y. Ma, *IEEE*

- Trans. Appl. Supercond. **7**, 2780 (1997).
- ²⁹K. T. Leong, J. C. Booth, and J. H. Claassen, J. Supercond. Nov. Magn. **19**, 637 (2006).
- ³⁰N. D. Orloff, J. Mateu, A. Lewandowski, E. Roca, J. King, D. Gu, X. Lu, C. Collado, I. Takeuchi, and J. C. Booth, IEEE Trans. Microw. Theory Tech. **59**, 188 (2011).
- ³¹L. Ranzani, L. Spietz, Z. Popovic, and J. Aumentado, IEEE Trans. Appl. Supercond. **22**, 1500606 (2012).
- ³²L. Spietz, K. Irwin, M. Lee, and J. Aumentado, Appl. Phys. Lett. **97**, 142502 (2010).
- ³³D. H. Slichter, Ph.D. thesis, University of California, Berkeley, 2011.
- ³⁴<http://web.physics.ucsb.edu/~martinigroup/electronics.shtml>.
- ³⁵J. Juroshek, IEEE Trans. Microw. Theory Tech. **35**, 457 (1987).
- ³⁶T. E. MacKenzie and A. E. Sanderson, IEEE Trans. Microw. Theory Tech. **14**, 29 (1966).
- ³⁷J. P. Hoffmann, P. Leuchtmann, and R. Vahldieck, Proc. European Microwave Conference, 388 (2007).
- ³⁸G. Vandersteen, Y. Rolain, J. Schoukens, and A. Verschueren, IEEE Trans. Microw. Theory Tech. **45**, 1027 (1997).
- ³⁹S. Ree and L. E. Reichl, Phys. Rev. E **60**, 1607 (1999).
- ⁴⁰B. Dietz, A. Heine, A. Richter, O. Bohigas, and P. Leboeuf, Phys. Rev. E **73**, 035201(R) (2006).
- ⁴¹B. Dietz, T. Friedrich, H. L. Harney, M. Miski-Oglu, A. Richter, F. Schäfer, and H. A. Weidenmüller, Phys. Rev. E **78**, 055204 (2008).
- ⁴²A. Richter, Phys. Scr. **T90**, 212 (2001).